Journal of Power Sources 184 (2008) 77–83

Contents lists available at ScienceDirect

Journal of Power Sources

journal homepage: www.elsevier.com/locate/jpowsour

Thermal, mechanical and phase stability of $LaCoO_3$ in reducing and oxidizing environments

M. Radovic[a], S.A. Speakman[b], L.F. Allard[b], E.A. Payzant[b], E. Lara-Curzio[b], W.M. Kriven[c], J. Lloyd[d], L. Fegely[d], N. Orlovskaya[e,*]

[a] Department of Mechanical Engineering, Texas A&M University, College Station, TX 77843, United States
[b] Materials Science and Technology Division, Oak Ridge National Laboratory, Oak Ridge, TN 37831, United States
[c] Department of Materials Science and Engineering, University of Illinois at Urbana-Champaign, Urbana, IL 61820, United States
[d] Department of Materials Science and Engineering, Drexel University, Philadelphia, PA 19104, United States
[e] Department of Mechanical, Materials and Aerospace Engineering, University of Central Florida, Orlando, FL 32816, United States

ARTICLE INFO

Article history:
Received 23 April 2008
Received in revised form 24 May 2008
Accepted 26 May 2008
Available online 22 July 2008

Keywords:
Reduction
Perovskite
Thermal expansion
Stability
Fuel cells

ABSTRACT

Thermal, mechanical, and phase stability of $LaCoO_3$ perovskite in air and 4% H_2/96% Ar reducing atmosphere have been studied by thermal mechanical analysis (TMA), high temperature microhardness, and high temperature/room temperature X-ray diffraction. The thermal behavior of $LaCoO_3$ in air exhibits a non-linear expansion in the 100–400 °C temperature range. A significant increase of coefficient of thermal expansion (CTE) measured in air both during heating and cooling experiments occurs in the 200–250 °C temperature range, corresponding to a known spin state transition. $LaCoO_3$ is found to be highly unstable in a reducing atmosphere. In case where $LaCoO_3$ was present as a powder, where surface reduction mechanism would prevail, the reduction starts as earlier as 375 °C with a formation of the metallic Co and La_2O_3 at 600 °C. In the bulk form, $LaCoO_3$ undergoes a series of expansion and contractions due to phase transformations beginning around 500 °C with very intensive chemical/phase changes at 800 °C and above. These expansions and contractions are directly related to the formation of $La_3Co_3O_8$, La_2CoO_4, $La_4Co_3O_{10}$, La_2O_3, CoO, and other Co compounds in the reducing atmosphere. Although $LaCoO_3$ is a good ionic and electronic conductor and catalyst, its high thermal expansion as well as structural, mechanical, and phase instability in reducing environments present a serious restriction for its application in solid oxide fuel cells, sensors or gas separation membranes.

1. Introduction

Lanthanum cobaltite, $LaCoO_3$, belongs to a family of mixed electronic and oxide-ion conducting perovskites that are good candidate materials for catalysts, oxygen separation membranes, solid oxide fuel cell cathodes, and oxygen sensors. $LaCoO_3$ is also of more fundamental interest because Co(III) ions undergo a transition with increasing temperature from the low-spin (LS) state t^6e^0 to the intermediate spin (IS) state t^5e^1 in the 35–320 K temperature range, and finally to a conductive state near 500 K in which conductive electrons occupy itinerant-electron states of a σ^* band of e-orbital parentage [1–3]. Several review papers [4–6] have been published on structural phenomena associated with the spin state transition in $LaCoO_3$.

$LaCoO_3$ has a high average coefficient of thermal expansion (CTE) of about $23 \times 10^{-6}\,K^{-1}$ over the 25–1000 °C temperature range. Thermal expansion of $LaCoO_3$ during heating in air depends on lattice expansion due to anharmonicity of lattice vibrations, spin states changes of Co^{3+} ion, and increase in oxygen vacancies concentration leading to chemical expansion [4]. When $LaCoO_3$ is exposed to a reducing environment, oxygen vacancies form in much larger quantities than when heated in air, especially at elevated temperatures, and the charge neutrality in the solid is maintained by the reduction of the transition metal on B-site to a lower valence state. This results in the increase of the average ionic radius of the Co ion, and consequent lattice expansion. It is also possible that oxygen vacancies in the ionic sublattice induce a columbic repulsion between the neighboring B-site cations that, in turn, results in additional expansion of the crystal lattice [7–9].

The $LaCoO_3$ is easily reduced up to metallic Co^0 via a number of different reduction steps with an overall reaction [10,11]:

$$2LaCoO_3 = La_2O_3 + 2Co + 3O_2$$

* Corresponding author. Tel.: +1 4078235770; fax: +1 4078230208.
E-mail address: norlovsk@mail.ucf.edu (N. Orlovskaya).

0378-7753/$ – see front matter © 2008 Elsevier B.V. All rights reserved.
doi:10.1016/j.jpowsour.2008.05.063

The details of reduction mechanism of $LaCoO_3$ remain ambiguous. While some papers reported one-step reduction of Co^{3+} in $LaCoO_3$ to Co^0 phase [11,12], other reported an oxygen deficient intermediate $LaCoO_{3-\delta}$ structures where Co^{3+} is reduced first to Co^{2+} and further to Co^0 via two-step process [13,14]. Due to its easy reducibility $LaCoO_3$ is of considerable interest for redox catalyst, such as hydrogenation of ethylene [15], the hydrogenolysis of ethane and ethane/C_3–C_5 alkanes on the perovskite surface [16], and others [17,18]. However, as a part of the oxygen separation membrane, $LaCoO_3$ could compromise the durability and reliability of the complex perovskite membrane reactors due to lack of dimensional, mechanical, and phase stability.

In this paper, we report on thermal expansion of $LaCoO_3$ in reducing (4% H_2/96% Ar or N_2) and oxidizing (air) environments as determined by thermal mechanical analysis (TMA). Degradation of mechanical properties of $LaCoO_3$ was studied by Vickers indentation as a function of temperature in the reducing atmosphere. Dimensional changes during reduction of $LaCoO_3$ by hydrogen were studied by isothermal TMA while phase compositions at different stages of the reduction were determined by X-ray powder diffraction (XRD). Both surface and bulk reduction mechanisms occurring under harsh H_2/inert gas reduction conditions are reported.

2. Experimental procedure

$LaCoO_3$ samples were produced by Praxair Surface Technologies, Specialties Ceramics. The samples were sintered at 1350 °C for 2 h in air and machined into 3 mm × 3 mm × 6 mm bars. As confirmed by XRD, the samples were 99% pure $LaCoO_3$ with minor traces of secondary phases (Table 1). The porosity of the sintered samples was 6–7% as measured by the Archimedes method.

A thermal mechanical analyzer, TMA (TMA Q400, TA Instruments, New Castle, DE) was used to characterize the thermal properties of samples, notably the thermal expansion. The TMA rests a quartz probe on the upper surface of the sample and the probe is supported on an air bearing. As the sample heats in the furnace it expands, lifting the probe and the air bearing which is monitored by an optical transducer. To provide good contact between probe and specimen during the test, a small load of 0.5 N was applied on the specimen via a quartz probe. Thermal expansion measurements were carried out using 3 mm × 3 mm × 6 mm $LaCoO_3$ samples in ambient air and 4% H_2/96% Ar in the temperature range of 25–1000 °C with a heating/cooling rate of 10 °C min^{-1}. In addition, the thermal expansion of $LaCoO_3$ during isothermal heating at 850 °C in a reducing atmosphere of 4% H_2/96% Ar for different times was also studied. For the isothermal dwelling, the sample was first heated in air up to 850 °C with a heating rate of 3 °C min^{-1}. The air was replaced by 4% H_2/96% Ar gas when temperature reached 850 °C. After the isothermal dwelling was complete at a given time, the sample was fast cooled inside the furnace and taken for further scanning electron microscopy (SEM) and XRD studies.

The coefficient of linear thermal expansion is defined as the ratio of the change in length per unit length per unit change in temperature [19]. The length of the specimen (L) can be expressed as a function of temperature using following equation:

$$L = L_0(1 + \alpha\,\Delta T) \tag{1}$$

where L is the specimen's length at T_1, L_0 is the length at T_0, and α is the coefficient of linear thermal expansion and $\Delta T = T_1 - T_0$. Usually an average CTE is determined and used over the temperature range of interest, when thermal expansion changes more or less linearly with temperature. However, CTE at each temperature, the so-called instantaneous thermal expansion coefficient, can be calculated as the derivative of the relative length change versus temperature curve, i.e. using following relation:

$$\alpha = \frac{1}{L_0}\frac{dL}{dT} \tag{2}$$

In this work we calculated instantaneous CTEs of $LaCoO_3$ heated both in air and in 4% H_2/96% Ar. To calculate the derivative, the recorded dependence of $(L - L_0)$ as a function of T was approximated by a sixth-order polynomial in order to obtain smooth curve fit to the experimental data. The polynomial was differentiated analytically, and the derivative was calculated.

Scanning electron microscopy along with energy dispersive spectroscopy (EDS) was carried out on selected $LaCoO_3$ specimens before and after reduction using Hitachi S-4700 field emission scanning electron microscope.

High-temperature X-ray diffraction (HTXRD) data were collected using a PANalytical X'Pert PRO MPD diffractometer with an Anton-Paar XRK-900 high temperature stage. The diffractometer was equipped with an X'Celerator detector that allows fast data collection. The data were collected using Cu Kα radiation at 45 kV and 40 mA. Data were collected between 10° and 80° 2θ with a count time of 30 s so that each scan took less than 5 min. In situ heating of $LaCoO_3$ powder was performed with 10 °C min^{-1} heating rate up to 900 °C in 4% H_2/96% N_2 atmosphere to collect high temperature XRD data.

Room temperature X-ray powder diffraction measurements of the crushed $LaCoO_3$ bars before and after different degrees of reduction were conducted using a Scintag PAD V vertical $\theta/2\theta$ goniometer with Cu Kα radiation (45 kV and 40 μA) and a Si(Li) Peltier-cooled solid-state detector through a 10–80° 2θ range with a 0.02° angular step and a collection time of 8 s per step. The ambient temperature during data collection was 298 ± 1 K. The specimens were prepared by making a slurry mixture of sample powder and methanol and spreading the slurry on a quartz zero background plate. JADE (Materials Data, Inc.) software and the PDF4+ database (ICDD, 2007) were used to identify XRD peaks. High Score Plus (PANalytical, Inc.) software was used to quantitatively analyze the different phases in the mixture of compounds following reduction.

The high temperature microhardness was determined using a Nikon Model QM High Temperature Microhardness Tester (Nikon, Japan) at a load of 200 g (1.962 N) and a dwell time of 10 s. The oxygen partial pressure inside the microhardness tester was kept at 5×10^{-5} Pa to ensure the reducing atmosphere during the indentation test.

3. Results and discussion

3.1. High temperature thermal stability in air and in 4% H_2/96% Ar

Fig. 1a shows the thermal expansion of $LaCoO_3$ upon heating and corresponding thermal contraction of the samples upon cooling in air, while Fig. 1b shows corresponding changes of instantaneous CTE with temperature that was calculated from Fig. 1a using Eq. (2). As it is expected the shrinkage of the sample upon cooling and expansion during heating curves almost overlap with the exception that the small hysteresis occurs in the high temperature region. The difference in thermal expansion upon heating and cooling in the high temperature region can be explained by the intensive oxygen vacancies formation on heating and the resulting different oxygen stoichiometry upon cooling. Not surprisingly, the instantaneous CTE versus temperature curves during heating and cooling (Fig. 1b) closely match. Three distinctive segments on the sigmoid CTE versus temperature curves can be observed in Fig. 1b. The first one is in the 25–230 °C temperature range where CTE increases from 12×10^{-6} to 28.7×10^{-6} K^{-1}. After it reaches the maximum value at 230 °C, the instantaneous CTE decreases to

Table 1
Phase composition of the material upon reduction of $LaCoO_3$ in H_2/Ar

Point #	1, 2	3	4	5	6
Reduction time (min)	0	88	172	325	2211
Environment	Air	4% H_2/96% Ar	4% H_2/96% Ar	4% H_2/96% Ar	4% H_2/96% Ar
Temperature (°C)	22–850	850	850	850	850
Content of phase (wt%)					
$LaCoO_3$[a]	100	81.8	19.5	–	–
$La_3Co_3O_8 + La_2Co_2O_5$	–	11.3	0.2	–	–
$La_4Co_3O_{10}$	–	8.4	62.9	0.5	–
La_2CoO_4	–	–	10.2	76.9	62.9
CoO	–	0.5	7.1	16.1	1.9
La_2O_3[b]	–	–	–	3.2	23.2
Co_{cubic}	–	–	–	3.2	11.9

[a] Traces (<0.5%) of La (or LaCo alloy) were identified in $LaCoO_3$ perovskite.
[b] The calculated quantities include $La(OH)_3$ hydroxide.

20×10^{-6} to $21 \times 10^{-6}\,K^{-1}$ at 600 °C. Above that temperature CTE remains almost constant and does not change with temperature.

Comparatively high CTE values of $LaCoO_3$ in a 25–230 °C temperature range can be explained by a thermal population of the intermediate spin state of Co^{3+} ions that exists because of the magnetic phase transition in $LaCoO_3$ from low to intermediate spin state at low temperature. However, the nature of the sigmoid CTE versus temperature curve is not completely understood since the existence of intermediate spin state Co^{3+} ions cannot explain the significant maximum in CTE at 230 °C. The different explanations for the appearance of the peak CTE value are proposed, such as change in orbital ordering [20] or a second-order phase transition from semiconducting to metallic state [21]. It is not clear at this point which of these mechanisms is the dominant one for the observed thermal expansion anomaly in the 25–500 °C temperature range.

The thermal expansion of the $LaCoO_3$ in a reducing atmosphere (4% H_2/96% Ar) (Fig. 1c and d) is different than expansion in air (Fig. 1a and b). While at low temperatures, up to 450–500 °C, thermal behavior of $LaCoO_3$ in reducing and oxidizing environments during heating are essentially the same. However, starting from 550 °C a significant increase in CTE is observed that reaches a maximum of $\sim 25 \times 10^{-6}\,K^{-1}$ at temperature of 780 °C above which it decreases again with temperature. The instantaneous CTE versus temperature curve obtained upon cooling in reduced atmosphere is significantly different than those obtained during heating in reduced environment and heating and cooling in air. CTE decreased from about $31.5 \times 10^{-6}\,K^{-1}$ at 900 °C to $9 \times 10^{-6}\,K^{-1}$ at 780 °C and up to RT upon cooling. Then CTE increases or decreases again with decrease in temperature and reaches two local maxima, first of $13 \times 10^{-6}\,K^{-1}$ at 570 °C and the second one of $14 \times 10^{-6}\,K^{-1}$ at 180 °C. The deviation of the CTE versus temperature curves obtained in reduced environment upon heating and cooling from those that were obtained during heating in reducing environment or heating and cooling in air can be explained by (a) vacancy formation and

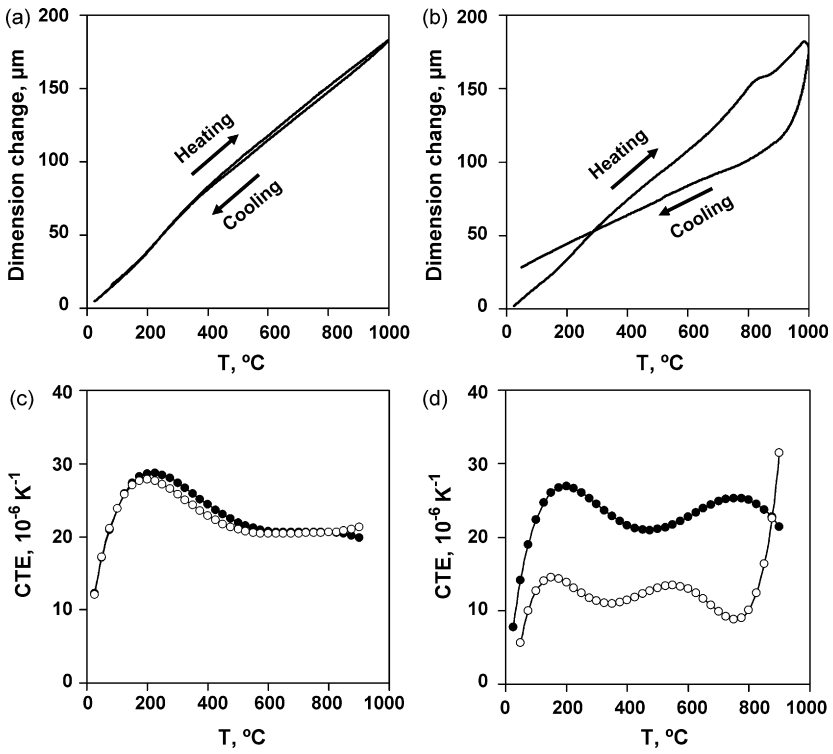

Fig. 1. Thermal expansion (a) and instantaneous coefficient of thermal expansion (b) of $LaCoO_3$ in air as a function of temperature. Thermal expansion (c) and instantaneous coefficient of thermal expansion (d) in 4% H_2/96% Ar gas mixture as a function of temperature. Closed circles in (b) and (d) correspond to heating while opens circles correspond to cooling regime.

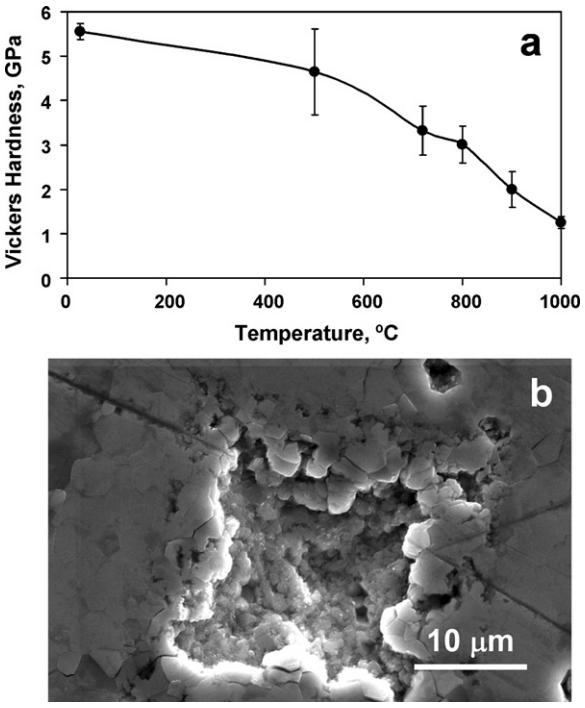

Fig. 2. High temperature Vickers hardness (a) of $LaCoO_3$ perovskite. The measurements were performed in vacuum. SEM of the impression (b) made at the $LaCoO_3$ surface at 1000 °C.

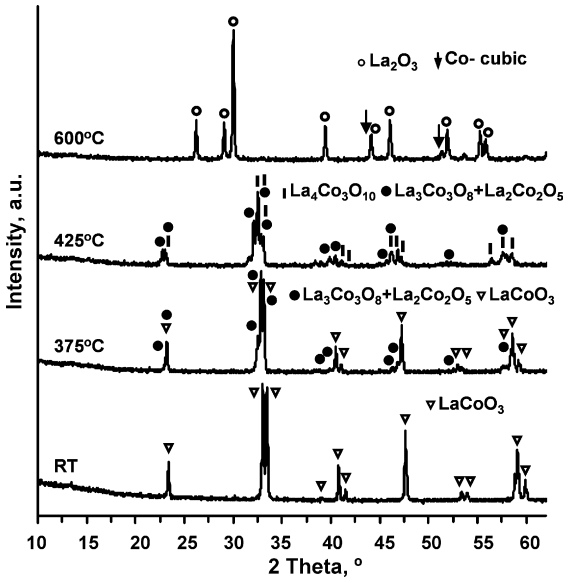

Fig. 3. XRD pattern of $LaCoO_3$ powder showing the reduction steps of the cobaltite upon heating in 4% H_2/96% N_2 atmosphere. PDF card numbers used to identify the compounds are as follows: 00-048-0123 for $LaCoO_3$; 01-089-1319 for $La_3Co_3O_8$; 01-070-2701 for $La_2Co_2O_5$; 00-034-1150 for $La_4Co_3O_{10}$; 00-015-0806 for Co; 00-05-0602 for La_2O_3.

(b) reduction of $LaCoO_3$ and formation of other phases (see below) during heating in reducing atmosphere.

3.2. Mechanical and phase stability during reduction

It is well established the $LaCoO_3$ reduces easily in a reducing environments [11–13]. Such reducibility is detrimental for the mechanical stability of the perovskites. The deleterious effect of reduction on the mechanical properties of $LaCoO_3$ can be illustrated by the changes of hardness as function of temperature in reducing environments. Fig. 2 shows high temperature hardness of $LaCoO_3$ measured during the heating of the ceramic in vacuum with oxygen partial pressure of 5×10^{-5} Pa. While there is a decrease of hardness starting from 600 °C, the significant deterioration of hardness starts at around 800 °C, which approximately coincides with changes observed in the thermal expansion due to structural changes in the reducing atmosphere.

The changes in thermal expansion and mechanical properties of $LaCoO_3$ in reducing environments can be understood from the changes in the phase composition. In situ X-ray diffraction of $LaCoO_3$ powders heated in H_2/Ar atmosphere as shown in Fig. 3 reveals a rapid reduction of $LaCoO_3$ starting at temperatures as low as 375 °C with formation of oxygen deficient brownmillerite $La_3Co_3O_8$ and $La_5Co_2O_5$ phases. Upon further reduction, the amount of $La_3Co_3O_8$ and $La_2Co_2O_5$ phases grow over the 375–425 °C temperature range. The $La_4Co_3O_{10}$ phase was formed upon further heating at 425 °C until the material was finally reduced to La_2O_3 and metallic Co at 600 °C. These two phases remained stable through the full sequence of heating/cooling steps up to 900 °C in H_2/Ar. It is important to notice that such rapid reduction process was possible because of the prevalence of surface reduction of $LaCoO_3$ powder, as opposed to the bulk reduction of 3 mm × 3 mm × 6 mm bars of cobaltite described in Section 3.3 below.

3.3. Stability during isothermal reduction in H_2

As it can be seen from Fig. 1c, the most dramatic dimensional changes in reducing environment occurred at about 830–850 °C where a significant deviation from linear expansion of $LaCoO_3$ with temperature has been observed during TMA measurements. In order to clarify the structural changes in $LaCoO_3$ upon H_2 reduction and their effect on expansion, the sample was heated first in air up to 850 °C at the rate of 3 °C min^{-1} (Point #1, Fig. 4a). Once the temperature of 850 °C was reached, a 4% H_2/96% Ar gas mixture was introduced in the TMA chamber (Point #2, Fig. 4a) and temperature was kept constant. During the isothermal heating at 850 °C in the reducing atmosphere the sample expanded from $\Delta L/L = 1.8\%$ up to $\Delta L/L = 2.1\%$ (Point #3, Fig. 4a). After that point the sample shrank until the minimal point $\Delta L/L = 1.8\%$ was reached (Point #4, Fig. 4a). However, after that point it expanded again up to $\Delta L/L = 2.25\%$ (Point #5, Fig. 4a). Upon further dwelling for the total 72 h significant contraction of the sample has been observed.

To clarify the nature of the structural changes of $LaCoO_3$ upon reduction at these specific isothermal conditions, we performed three experiments where the $LaCoO_3$ samples were treated in the same way as in the first TMA run except that the reduction process was stopped at specific points of interest (Points #3–5 in Fig. 4a) and the sample was quickly cooled down to room temperature. After fast cooling in the 4% H_2/96% Ar gas mixture to RT the samples were crushed and XRD patterns were taken. The phase compositions of five samples (Points #1 and #3–6 in Fig. 4) are presented in Fig. 5. Before reduction the primary phase was $LaCoO_3$ rhombohedral perovskite with only trace of secondary phases (Table 1).

The reduction of $LaCoO_3$ in H_2/Ar for 88 min (Point #3, Fig. 4a) yields a mixture of $LaCoO_3$ and at least two deformed oxygen deficient perovskite related structures—$La_3Co_3O_8$ [22] and $La_2Co_2O_5$ [23] phases that were formed as a result of the following chemical reactions:

$$6LaCoO_3 \rightarrow 2La_3Co_3O_8 + O_2\uparrow$$

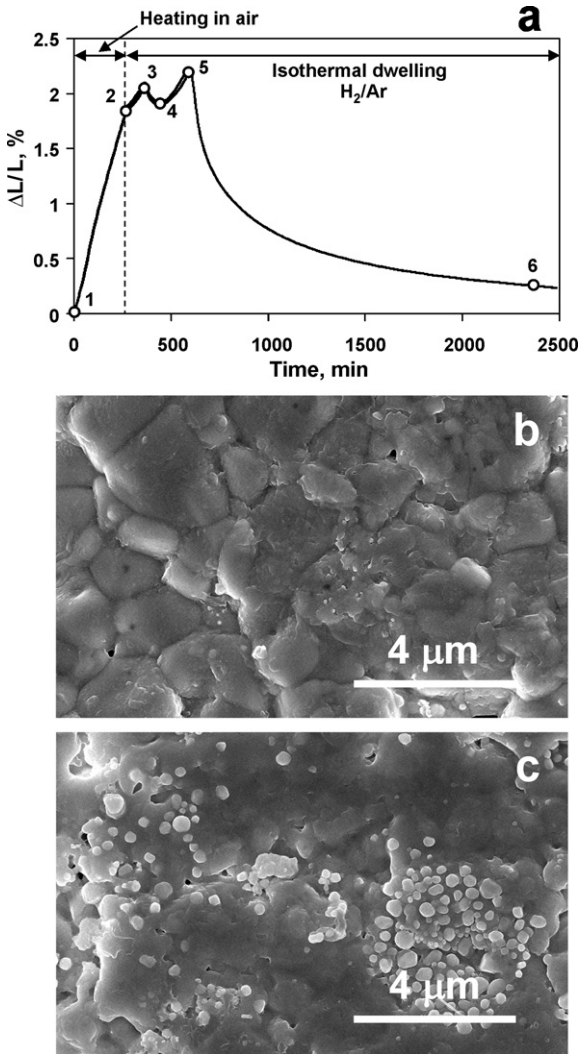

Fig. 4. (a) Thermal expansion of $LaCoO_3$ ceramics upon isothermal dwelling in 4% H_2/96% Ar atmosphere; (b) SEM image of $LaCoO_3$ surface after isothermal dwelling at 850 °C in 4% H_2/96% Ar for 88 min; (c) SEM image of $LaCoO_3$ surface after isothermal dwelling at 850 °C in 4% H_2/96% Ar for 2211 min. The white spherical particles found on the sample surface consist of the Co-rich phase, as found by EDS, most likely they are metallic Co precipitates formed during severe reduction.

followed by

$$4La_3Co_3O_8 \rightarrow 6La_2Co_2O_5 + O_2\uparrow$$

The brownmillerite-type structures of $La_3Co_3O_8$ and $La_2Co_2O_5$ consist of alternate layers of Co in octahedral and tetrahedral sites. The structure may be derived from the perovskite-type structure by removing rows of oxygen atoms from alternate planes. Every second row of oxygen atoms is removed in $La_2Co_2O_5$. The main feature which accompanied the formation of oxygen deficient perovskite-related phases is a significant thermal/chemical expansion (Points #2–3 in Figs. 4a and 5). The expansion at the recent stages of oxygen removal from the perovskite lattice is well documented in the literature [8,24]. SEM micrograph shows the etched surface of the cobaltite sample, the grains are clearly visible, after isothermal dwelling at 850 °C for 88 min in H_2/Ar (Fig. 4b).

Vacancy formation can also contribute to the initial expansion at the isothermal dwelling of the $LaCoO_3$ in the reducing environment at 850 °C. Each extra vacancy is associated with an increase in the lattice parameter of the oxide crystal due to the appearance of the repulsive forces between atoms in the perovskite, therefore, the lattice expands as the oxide become more nonstoichiometric. The ionic radius for Co increases from 61 pm (Co^{III}) to 67 pm (Co^{II}) which in turn also contributes to the expansion of the perovskite-type lattice. At certain point of oxygen removal from the lattice the topotactic reduction to vacancy-ordered phases $La_3Co_3O_8$ and further to $La_2Co_2O_5$ occurred.

Further increase in oxygen deficiency in the reducing environment leads to the collapse of perovskite and brownmillerite structures. The phase transformation from perovskite and brownmillerite structures to $La_4Co_3O_{10}$, La_2CoO_4 and CoO takes place (Points #3–4 in Figs. 4a and 5, reduction in H_2/Ar for 172 min) as a result of following chemical reactions:

$$8LaCoO_3 \rightarrow 2La_4Co_3O_{10} + 2CoO + O_2\uparrow$$

$$4LaCoO_3 \rightarrow 2La_2CoO_4 + 2CoO + 3O_2\uparrow$$

$$La_2Co_2O_5 \rightarrow La_2CoO_4 + CoO$$

The $La_4Co_3O_{10}$ ($LaO(LaCoO_3)_3$) is an intermediate product of reduction between $LaCoO_3$ and La_2CoO_4 ($LaO(LaCoO_3)$). It is considered a member of the $AO(ABO_3)_n$ ternary compounds. Three members of the group were reported in La–Co–O system: $LaCoO_3$ ($n=\infty$), La_2CoO_4 ($n=1$) orthorhombic with K_2NiF_4-type structure, and $La_4Co_3O_{10}$ ($n=3$). The structure of $AO(ABO_3)_n$ contains n perovskite sheets separated by an AO sheet of NaCl-like structure [25,26]. The crystal structures of these phases are of Ruddlesden–Popper type [27]. This type of structure can ideally be described by the stacking of n two-dimensional perovskite-type sheets of corner-sharing CoO_6-octahedra along the crystallographic c-direction into layers $(LaCoO_3)_n$, which are separated by a single LaO layer [23].

During further reduction for up to 325 min in H_2/Ar gas mixture (Points #4–5 in Figs. 4a and 5) $La_4Co_3O_{10}$ is reduced to lanthanum oxide La_2O_3 and cobalt oxide Co_3O_4 with spinel structure, and La_2CoO_4 is reduced to La_2O_3 and cobalt oxide CoO. All three oxides have been found after reduction of $LaCoO_3$ in H_2/Ar for 325 min (Fig. 5). Neither $LaCoO_3$ nor $La_4Co_3O_{10}$ was detected after isothermal reduction for 325 min (Point #5 in Fig. 4a) as it is shown in Table 1. The reduction process at this stage can be possibly expressed as:

$$La_4Co_3O_{10} \rightarrow 2La_2O_3 + Co_3O_4$$

followed by

$$2Co_3O_4 \rightarrow 6CoO + 3O_2\uparrow$$

and

$$La_2CoO_4 \rightarrow La_2O_3 + CoO$$

After being reduced for 72 h at 850 °C (Point #6), Co phase has been found along with CoO, La_2O_3 and La_2CoO_4 oxide as a major phase is present. SEM has revealed the formation of Co particles at the surface of the reduced sample after 72 h of dwell at 850 °C (Fig. 4c). An oxidation state of the cobalt oxide in air varies at about 861 °C [28]. The final stages of the reduction process can be written as:

$$2CoO \rightarrow 2Co + O_2\uparrow$$

Lanthanum hydroxide $La(OH)_3$ has been also found because of the highly hydroscopic nature of La_2O_3 oxide. The formation of lanthanum hydroxide can be explained by partial hydration of La_2O_3 in humid air at ambient temperature between the high temperature

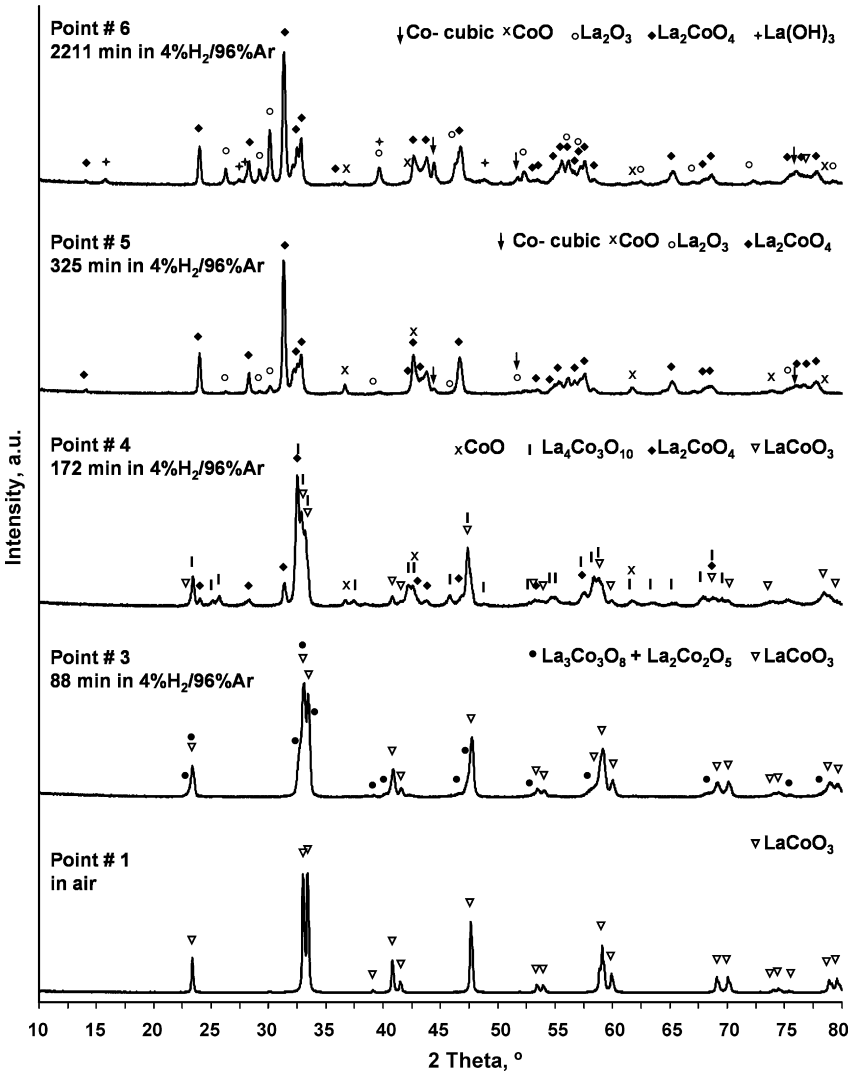

Fig. 5. XRD patterns of $LaCoO_3$ ceramics taken after isothermal heating in 4% H_2/96% Ar atmosphere at different reduction steps. PDF card numbers used to identify $La(OH)_3$ was 00-036-1481. Other PDF cards are listed in Fig. 3 caption.

reduction and room temperature XRD through following chemical reaction:

$$La_2O_3 + 3H_2O \rightarrow 2La(OH)_3$$

The fraction of hydroxides to oxide increases over time, depending on the ambient humidity.

Phase fractions for each phase present in the sample at different reduction stages of $LaCoO_3$ perovskite are presented in Table 1. The perovskite surface after reduction was significantly affected by the reducing atmosphere. Grains with clear grain boundaries, similar to the thermally etched grains, can be seen after heating at 850 °C for 88 min in H_2/Ar (Point #3a) (Fig. 4a). After reduction for 72 h (Point #6), the surface structure has been drastically changed and the spherical metal particles, rich in Co, can be seen (Fig. 4b).

4. Conclusion

A thermal expansion of $LaCoO_3$ have been measured from room temperature to 1000 °C in air and in 4% H_2/96% Ar and the instantaneous coefficient of thermal expansion has been calculated. The high CTE values with the sigmoid-type curve in the range of 100–500 °C are reported for the $LaCoO_3$ heated and cooled in air. The heating in the reducing environment (4% H_2/96% Ar) results in the reduction of $LaCoO_3$, especially at temperatures higher than 800 °C, and the irreversible structural changes occurring during reduction are responsible for a significant increase that is followed by further decrease of CTE with increasing temperature.

The reduction of $LaCoO_3$ has a drastic effect on the mechanical performance of the material, i.e. the hardness significantly decreases from 5.5 GPa measured at room temperature to ~1 GPa at 1000 °C in vacuum.

The structural changes affecting the thermal expansion of the $LaCoO_3$ during the isothermal dwelling under the reducing atmosphere have been identified. It was found that upon reduction at constant temperature 850 °C, the following structural changes have occurred: $LaCoO_3$ was reduced to $La_3Co_3O_8$ and further to $La_2Co_2O_5$ brownmillerite structures, with further reduction to even more oxygen deficient structures as $La_4Co_3O_{10}$ and La_2CoO_4 with simultaneous CoO precipitation. After the reduction for 72 h the mixture of two metallic Co phases along with CoO, La_2O_3 and La_2CoO_4 major phases can be found.

Acknowledgements

This research was supported by NSF, DMR (project #0201770) and in part by an appointment to the Department of Energy's Faculty and Student Team program. This research was also supported in part by the Assistant Secretary for energy efficiency and renewable energy, Office of FreedomCAR and Vehicle Technologies, as a part of the High Temperature Materials Laboratory User Program, Oak Ridge National Laboratory, managed by UT-Battelle, LLC, for the US Department of Energy under contract 2005-080 and 2003-059.

References

[1] J. Goodenough, J.-S. Zhou, Struct. Bond. 98 (2001) 17–113.
[2] G. Maris, Y. Ren, V. Volotchaev, C. Zobel, T. Lorenz, T.T.M. Palstra, Phys. Rev. B 67 (2003) 224423-1–224423-5.
[3] O. Haas, R.P.W. Struis, J.M. McBreen, J. Solid State Chem. 177 (2004) 1000–1010.
[4] P.G. Radaelli, S.-W. Cheong, Phys. Rev. B 66 (2002) 094408-1–094408-9.
[5] P. Ravindra, P.A. Korzhavyi, H. Fjellvag, A. Kjekshus, Phys. Rev. B 60 (1999) 16423–16434.
[6] P. Ravinsran, H. Fjellvag, A. Kjekshus, P. Blaha, K. Schwarz, J. Luitz, J. Appl. Phys. 91 (2002) 291–303.
[7] S. Miyoshi, J.-O. Hong, K. Yashiro, A. Kaimai, Y. Nigara, K. Kawamura, T. Kawada, J. Mizusaki, Solid State Ionics 161 (2003) 209–217.
[8] A. Atkinson, T.M.G.M. Ramos, Solid State Ionics 129 (2000) 259–269.
[9] S. Adler, J. Am. Ceram. Soc. 84 (2001) 2117–2119.
[10] L. Bedel, A.C. Roger, C. Estournes, A. Kienemann, Catal. Today 85 (2003) 207–218.
[11] L.B. Sis, G.P. Wirtz, S.C. Sorenson, J. Appl. Phys. 44 (1973) 5553–5559.
[12] L. Huang, M. Bassir, S. Kaliaguine, Appl. Surf. Sci. 243 (2005) 360–375.
[13] M. Crespin, W.K. Hall, J. Catal. 69 (1981) 359–370.
[14] T. Nakamura, G. Petzow, L.J. Gauckler, Mater. Res. Bull. 14 (1979) 649–659.
[15] J.O. Petunchi, J.L. Nicastro, E.A. Lombardo, J. Chem. Soc. Chem. Commun. (1980) 467–468.
[16] K. Ichimura, Y. Inoue, I. Yasumori, Bull. Chem. Soc. Jpn. 53 (1980) 3044.
[17] R.J.H. Voorhoeve, J.P. Remeika, P.E. Freeland, B.T. Matthias, Science 177 (1972) 353–354.
[18] H. Park, H.-P. Lee, Bull. Korean Chem. Soc. 9 (1988) 283–288.
[19] H.P. Kirchner, Progress in Solid State Chemistry, Macmilan, New York, 1964, p. 536.
[20] S. Uhlenbruck, F. Tietz, Mater. Sci. Eng. B 107 (2004) 277–282.
[21] D.I. Khomskii, G.A. Sawatzky, Solid State Commun. 102 (1997) 87–99.
[22] S. Stolen, F. Gronvold, H. Brinks, T. Atake, H. Mori, Phys. Rev. B 55 (1997) 14103–14106.
[23] K. Vidyasagar, A. Reller, J. Gapalakrishnan, C.N.R. Rao, J. Chem. Soc. Chem. Commun. (1985) 7–8.
[24] C.-Y. Tsai, A.G. Dixon, Y.H. Ma, W. Moser, M. Pascucci, J. Am. Ceram. Soc. 81 (1998) 1437–1444.
[25] O.H. Hansteen, H. Fjellvag, J. Solid State Chem. 141 (1998) 212–220.
[26] H. Fjellvag, O.H. Hansteen, B.C. Hauback, P. Fisher, J. Mater. Chem. 10 (2000) 749–754.
[27] S.N. Ruddlesden, P. Popper, Acta Cryst. 11 (1958) 54.
[28] G.V. Samsonov, The Oxide Handbook, 2nd edition, IFI/Plenum, Oxford, 1982.